

NON-MINIMALLY GRAVITY-COUPLED INFLATIONARY MODELS

C. PALLIS

*Physics Division, School of Technology,
Aristotle University of Thessaloniki,
GR-541 24 Thessaloniki, GREECE
kpallis@auth.gr*

ABSTRACT

We consider the non-supersymmetric models of chaotic (driven by a quadratic potential) and hybrid inflation, taking into account the minimal possible radiative corrections to the inflationary potential. We show that two simple coupling functions $f(\sigma)$ (with a parameter $c_{\mathcal{R}}$ involved) between the inflaton field σ and the Ricci scalar curvature ensure, for sub-Planckian values of the inflaton field, observationally acceptable values for the spectral index, n_s , and sufficient reheating after inflation. In the case of chaotic inflation we take $625 \lesssim c_{\mathcal{R}} \lesssim 2.1 \cdot 10^7$ resulting to $n_s \simeq 0.955$ and tensor-to-scalar ratio $r \simeq 0.2$. In the case of hybrid inflation, the selected $f(\sigma)$ assists us to obtain hilltop-type inflation. For values of the relevant mass parameter, m , less than 10^6 TeV and the observationally central value of n_s , we find $c_{\mathcal{R}} \simeq (0.015 - 0.078)$ with the relevant coupling constants $\lambda = \kappa$ and the symmetry breaking scale, M , confined in the ranges $(2 \cdot 10^{-7} - 0.001)$ and $(1 - 16.8) \cdot 10^{17}$ GeV, respectively.

1 INTRODUCTION

Non-minimal inflation (non-MI) [1] i.e., inflation constructed in the presence of a non-minimal coupling between the inflaton field and the Ricci scalar curvature, \mathcal{R} , has gained a fair amount of recent attention [2–4]. In particular, it is shown that non-MI can be realized within the *Standard Model* (SM) – or minimal extensions [5] of it – provided the inflaton couples strongly enough to \mathcal{R} . The role of inflaton can be played either by the Higgs doublet either by a SM singlet coupled to Higgs. Although quite compelling, non-MI within SM suffers from (i) several computational uncertainties regarding the impact of the quantum corrections in the presence of such a strong non-minimal gravitational coupling and (ii) the ambiguity about the hierarchy between the cutoff scale of the effective theory and the energy scale of the inflationary plateau [6–8]. Be that as it may, it would be interesting to examine if appropriately selected non-minimal gravitational couplings can have beneficial consequences for other well-motivated and rather natural models of inflation (for a relevant survey see, e.g., Ref. [9]).

Two such models are undoubtedly *Chaotic* (CI) [10] and *Hybrid Inflation* (HI) [11]. In this paper we focus on the non-supersymmetric version of these models. CI driven by a quadratic potential provides the simplest realization of inflation without initial-value problem and with quite interesting predictions for the (scalar) spectral index, n_s , and the scalar-to-tensor ratio, r . However, trans-Planckian inflaton-field values are typically required to allow for a sufficiently long period of inflation. Thus non-renormalizable corrections from quantum gravity are expected to destroy the flatness of the potential, invalidating thereby CI. On the other hand, HI – although can be accommodated with sub-Planckian values for the inflaton – suffers from the problem of the enhanced n_s which turns out to be, mostly, well above the prediction of the fitting [12] of the five-year results from the *Wilkinson Microwave Anisotropy Probe Satellite* (WMAP5) plus *baryon-acoustic-oscillations* (BAO) and *supernovae* (SN) data (for an up-to-date analysis of the problem of initial condition within HI, see Ref. [13]).

CONTENTS

1	INTRODUCTION	1
2	INFLATION WITH NON-MINIMAL GRAVITATIONAL COUPLING	2
2.1	NON-MINIMALLY CURVATURE-COUPLED SCALAR THEORY	3
2.2	INFLATIONARY OBSERVABLES – CONSTRAINTS	3
3	NON-MINIMAL CHAOTIC INFLATION	5
3.1	RESULTS FOR MCI	5
3.2	RESULTS FOR NON-MCI	5
4	NON-MINIMAL HYBRID INFLATION	7
4.1	RESULTS FOR MHI	8
4.2	RESULTS FOR NON-MHI	10
5	CONCLUSIONS	13
	REFERENCES	14

Note, in passing, that the introduction of *supersymmetry* (SUSY) and its local extension – supergravity (SUGRA) – can alleviate the shortcomings of both models – see Ref. [14] for several resolutions to the problem of CI and Ref. [15–19] for proposals related to the disadvantage of HI. However, we have to accept that there is no direct experimental confirmation of SUSY until now. On the contrary, there is a strong observational evidence in favor of the inflationary paradigm. Therefore, it is worthwhile to build inflationary models consistent with observations even without the presence of SUSY – for recent similar attempts, see Ref. [20, 21].

In this paper, we propose two types of non-minimal coupling functions $f(\sigma)$ between the inflaton and \mathcal{R} which support a resolution to the aforementioned problems of CI and HI. After the end of non-MI, both $f(\sigma)$'s shrink to unit assuring a safe transition to Einstein gravity in time. In the case of *non-minimal CI* (non-MCI) the inflationary potential is concave upwards and observationally exciting r 's are achieved. In the case of *non-minimal HI* (non-MHI) the inflationary trajectory is concave downwards and so, inflation turns out to be of hilltop-type [22]. In both cases, the minimal possible radiative corrections [23] to the inflationary potential are considered, sub-Planckian values of the inflaton field are required and adequate reheating of the universe is accomplished via curvature-induced [24] couplings of the inflaton to matter fields. Comparisons with the results obtained for the minimal version of both models are also displayed.

Below, we describe the generic formulation of non-MI (Sec. 2) and then apply the relevant results, for appropriate choices of $f(\sigma)$, in the case of non-MCI and non-MHI in Sec. 3 and 4 respectively. Finally, Sec. 5 summarizes our conclusions. Throughout the text, we set natural units for the Planck's constant, Boltzmann's constant and the velocity of light ($\hbar = c = k_B = 1$) the subscript χ denotes derivation *with respect to* (w.r.t.) the field χ (e.g., ${}_{,\chi\chi} = d^2/d\chi^2$) and a bar over a field χ denotes normalization w.r.t the reduced Planck mass, $m_P = 2.44 \cdot 10^{18}$ GeV, i.e., $\bar{\chi} = \chi/m_P$. Finally, we follow the conventions of Ref. [25] for the quantities related to the gravitational sector of our set-up.

2 INFLATION WITH NON-MINIMAL GRAVITATIONAL COUPLING

Non-MI, by its definition, can be realized by a scalar field non-minimally coupled to Ricci scalar curvature. The formulation of a such theory is described in Sec. 2.1. Based on it, we then derive the inflationary observables and impose observational constraints in Sec. 2.2.

2.1 NON-MINIMALLY CURVATURE-COUPLED SCALAR THEORY

The dynamics of a scalar field σ non-minimally coupled to \mathcal{R} through a coupling function $f(\sigma)$ is controlled, in the Jordan frame, by the following action – see, e.g., Ref. [4]:

$$\mathcal{S} = \int d^4x \sqrt{-g} \left(-\frac{1}{2} m_{\text{P}}^2 f(\sigma) \mathcal{R} + \frac{1}{2} g^{\mu\nu} \partial_\mu \sigma \partial_\nu \sigma - V(\sigma) \right), \quad (2.1)$$

where g is the determinant of the background Friedmann-Robertson-Walker metric [25]. To guarantee the validity of ordinary Einstein gravity at low energy, we require $f(\langle\sigma\rangle) = 1$, where $\langle\sigma\rangle$ is the *vacuum expectation value* (v.e.v) of σ at the end of non-MI.

The action in Eq. (2.1) can be brought in a simpler form by performing a conformal transformation [26] to the so-called Einstein frame where the the gravitational sector of our model becomes minimal. Indeed, if we define the Einstein-frame metric

$$\hat{g}_{\mu\nu} = f g_{\mu\nu} \Rightarrow \begin{cases} \sqrt{-\hat{g}} = f^2 \sqrt{-g} \text{ and } \hat{g}^{\mu\nu} = g^{\mu\nu} / f, \\ \hat{\mathcal{R}} = (\mathcal{R} + 3\Box \ln f + 3g^{\mu\nu} \partial_\mu f \partial_\nu f / 2f^2) / f \end{cases} \quad (2.2)$$

– where $\Box = (-g)^{-1/2} \partial_\mu (\sqrt{-g} \partial^\mu)$ and hat is used to denote quantities defined in the Einstein frame – and introduce the Einstein-frame canonically normalized field, $\hat{\sigma}$, and potential, \hat{V} , defined as follows:

$$\left(\frac{d\hat{\sigma}}{d\sigma} \right)^2 = J^2 = \frac{1}{f} + \frac{3}{2} m_{\text{P}}^2 \left(\frac{f_{,\sigma}}{f} \right)^2 \quad \text{and} \quad \hat{V}(\hat{\sigma}) = \frac{V(\hat{\sigma}(\sigma))}{f(\hat{\sigma}(\sigma))^2}, \quad (2.3)$$

the action in Eq. (2.1) can be simplified, taking the form

$$\mathcal{S} = \int d^4x \sqrt{-\hat{g}} \left(-\frac{1}{2} m_{\text{P}}^2 \hat{\mathcal{R}} + \frac{1}{2} \hat{g}^{\mu\nu} \partial_\mu \hat{\sigma} \partial_\nu \hat{\sigma} - \hat{V}(\hat{\sigma}) \right). \quad (2.4)$$

Based on the action above, we can proceed readily to the analysis of non-MI in the Einstein frame using the standard slow-roll approximation [9, 27] – see below. It can be shown [28] that the results calculated this way are the same as if we had calculated them with the non-minimally coupled scalar field in the Jordan frame.

One of the outstanding features of the scalar theories with non-minimal $f(\sigma)$ is that σ can decay via gravitational effects [24] even without explicit couplings between σ and matter fields. This is, because couplings arise spontaneously when σ settles in its v.e.v, $\langle\sigma\rangle$, and oscillates, with coupling constants involving derivatives of $f(\sigma)$ calculated for $\sigma = \langle\sigma\rangle$. If we identify σ as the inflaton, these couplings can ensure the reheating of the universe. Assuming the existence of a bosonic field minimally coupled to gravity, with negligible mass compared to the mass of σ , $m_\sigma = V_{,\sigma\sigma}(\langle\sigma\rangle)^{1/2}$, we get [24, 29] for the reheat temperature

$$T_{\text{rh}} \simeq \left(\frac{5\pi^2 g_{\rho*}(T_{\text{rh}})}{72} \right)^{-1/4} \sqrt{\Gamma_\sigma m_{\text{P}}} \quad \text{where} \quad \Gamma_\sigma \simeq \frac{f_{,\sigma}(\langle\sigma\rangle)^2 m_\sigma^3}{128\pi} \left(1 + \frac{3}{2} m_{\text{P}}^2 f_{,\sigma}(\langle\sigma\rangle)^2 \right)^{-1} \quad (2.5)$$

is the decay rate of σ , in the regime $T \ll m_\sigma$ which is valid in our applications. Clearly, this construction is applicable if $f_{,\sigma}(\langle\sigma\rangle) \neq 0$ (and this is valid for the f 's considered in Sec. 3 and 4). Also, assuming the particle spectrum of SM, we set $g_{\rho*} = 106.75$ for the relativistic degrees of freedom.

2.2 INFLATIONARY OBSERVABLES – CONSTRAINTS

Under the assumption that (i) the curvature perturbations generated by σ is solely responsible for the observed curvature perturbation and (ii) there is a conventional cosmological evolution (see below) after inflation, the inflationary parameters can be restricted imposing the following requirements :

(a) The power spectrum $P_{\mathcal{R}}$ of the curvature perturbations generated by σ at the pivot scale $k_* = 0.002/\text{Mpc}$ is to be confronted with the WMAP5 data [12],

$$P_{\mathcal{R}}^{1/2} = \frac{1}{2\sqrt{3}\pi m_{\text{P}}^3} \frac{\hat{V}(\hat{\sigma}_*)^{3/2}}{|\hat{V}_{,\hat{\sigma}}(\hat{\sigma}_*)|} = \frac{|J(\sigma_*)|}{2\sqrt{3}\pi m_{\text{P}}^3} \frac{\hat{V}(\sigma_*)^{3/2}}{|\hat{V}_{,\sigma}(\sigma_*)|} \simeq 4.91 \cdot 10^{-5}, \quad (2.6)$$

where $\sigma_* [\hat{\sigma}_*]$ is the value of $\sigma [\hat{\sigma}]$ when k_* crosses outside the inflationary horizon.

(b) The number of e-foldings, \hat{N}_* , that the scale k_* suffers during FHI is to account for the total number of e-foldings \hat{N}_{tot} required for solving the horizon and flatness problems of standard big bag cosmology, i.e., $\hat{N}_* = \hat{N}_{\text{tot}}$. Specifically, we calculate \hat{N}_* through the relation

$$\hat{N}_* = \frac{1}{m_{\text{P}}^2} \int_{\hat{\sigma}_{\text{f}}}^{\hat{\sigma}_*} d\hat{\sigma} \frac{\hat{V}}{\hat{V}_{,\hat{\sigma}}} = \frac{1}{m_{\text{P}}^2} \int_{\sigma_{\text{f}}}^{\sigma_*} d\sigma J^2 \frac{\hat{V}}{\hat{V}_{,\sigma}}, \quad (2.7)$$

where $\sigma_{\text{f}} [\hat{\sigma}_{\text{f}}]$ is the value of $\sigma [\hat{\sigma}]$ at the end of inflation, which can be found, in the slow-roll approximation and for the considered in this paper models, from the condition

$$\max\{\hat{\epsilon}(\sigma_{\text{f}}), |\hat{\eta}(\sigma_{\text{f}})|\} = 1, \quad \text{where}$$

$$\hat{\epsilon} = \frac{m_{\text{P}}^2}{2} \left(\frac{V_{,\hat{\sigma}}}{V} \right)^2 = \frac{m_{\text{P}}^2}{2J^2} \left(\frac{\hat{V}_{,\sigma}}{\hat{V}} \right)^2 \quad \text{and} \quad \hat{\eta} = m_{\text{P}}^2 \frac{V_{,\hat{\sigma}\hat{\sigma}}}{V} = \frac{m_{\text{P}}^2}{J^2} \left(\frac{\hat{V}_{,\sigma\sigma}}{\hat{V}} - \frac{\hat{V}_{,\sigma}}{\hat{V}} \frac{J_{,\sigma}}{J} \right). \quad (2.8)$$

The required \hat{N}_{tot} at k_* can be easily derived [19] consistently with our assumption of a conventional post-inflationary evolution. In particular, we assume that inflation is followed successively by the following three epochs: (i) the decaying-inflaton dominated era which lasts at a reheat temperature T_{rh} , (ii) a radiation dominated epoch, with initial temperature T_{rh} , which terminates at the matter-radiation equality, (iii) the matter dominated era until today. In particular, we obtain – c.f. Ref. [19]

$$\hat{N}_{\text{tot}} \simeq 22.4 + 2 \ln \frac{V(\sigma_*)^{1/4}}{1 \text{ GeV}} - \frac{4}{3} \ln \frac{V(\sigma_{\text{f}})^{1/4}}{1 \text{ GeV}} + \frac{1}{3} \ln \frac{T_{\text{rh}}}{1 \text{ GeV}} + \frac{1}{2} \ln \frac{f(\sigma_{\text{f}})}{f(\sigma_*)}, \quad (2.9)$$

where the last term emerges [7] from the transition from the Jordan to Einstein frame. Note that $\hat{R} = \sqrt{f}R$ with R being the scale factor of the universe.

(c) The (scalar) spectral index, n_{s} , its running, a_{s} , and the scalar-to-tensor ratio r are to be consistent with the fitting [12] of the WMAP5 plus BAO and SN data, i.e.,

$$(a) \quad n_{\text{s}} = 0.96 \pm 0.026, \quad (b) \quad -0.068 \leq a_{\text{s}} \leq 0.012 \quad \text{and} \quad (c) \quad r < 0.22, \quad (2.10)$$

at 95% confidence level (c.l.). The observable quantities above can be estimated through the relations:

$$n_{\text{s}} = 1 - 6\hat{\epsilon}_* + 2\hat{\eta}_*, \quad \alpha_{\text{s}} = \frac{2}{3} (4\hat{\eta}_*^2 - (n_{\text{s}} - 1)^2) - 2\hat{\xi}_* \quad \text{and} \quad r = 16\hat{\epsilon}, \quad (2.11)$$

where $\hat{\xi} = m_{\text{P}}^4 \hat{V}_{,\hat{\sigma}} \hat{V}_{,\hat{\sigma}\hat{\sigma}} / \hat{V}^2 = m_{\text{P}}^2 \hat{V}_{,\sigma} \hat{\eta}_{,\sigma} / \hat{V} J^2 + 2\hat{\eta}\hat{\epsilon}$ and the variables with subscript $*$ are evaluated at $\sigma = \sigma_*$. Note, in passing, that the utilized here non minimal $f(\sigma)$'s do not produce [30] observationally interesting non-gaussianity – for reviews see, e.g., Ref. [31].

(d) To avoid corrections from quantum gravity, we impose two additional theoretical constraints on our models – keeping in mind that $\hat{V}(\sigma_{\text{f}}) \leq \hat{V}(\sigma_*)$:

$$(a) \quad V(\sigma_*)^{1/4} \leq m_{\text{P}} \quad \text{and} \quad (b) \quad \sigma_* \leq m_{\text{P}}. \quad (2.12)$$

Although it is argued [20, 32] that violation of Eq. (2.12b) may not be necessarily fatal, we insist on imposing this condition in order to deliberate our proposal from our ignorance about the Planck-scale physics.

T_{rh} (GeV)	σ_*/m_{P}	m (10^{13} GeV)	n_s	α_s (10^{-4})	r
10^{10}	15.13	1.6	0.965	6.1	0.139
10^6	14.73	1.69	0.963	6.7	0.147
10^5	14.61	1.72	0.962	7	0.15
10^4	14.5	1.74	0.962	7.2	0.152

Table 1: Values of parameters allowed by Eqs. (2.7), (2.9) and (2.6) for MCI with several T_{rh} 's.

3 NON-MINIMAL CHAOTIC INFLATION

We focus on CI driven primarily by a quadratic potential of the form

$$V = \frac{1}{2}m^2\sigma^2 + V_{\text{rc}} \quad \text{where} \quad V_{\text{rc}} = \frac{1}{64\pi^2}m^4 \ln \frac{m^2}{Q^2} \quad (3.1)$$

are radiative corrections [23] to the inflationary potential. These are considered just for completeness since they have negligible impact on our results for any value of the renormalization scale, Q . We below recall (Sec. 3.1) the results for MCI (with $f(\sigma) = 1$) and describe (Sec. 3.2) our findings for non-MCI, adopting the following coupling function – recall that $\bar{\sigma} = \sigma/m_{\text{P}}$:

$$f(\sigma) = (1 + c_{\mathcal{R}}\bar{\sigma})^{-1}. \quad (3.2)$$

Note, in passing, that results for non-MCI with quartic potential are presented in Ref. [1, 33].

3.1 RESULTS FOR MCI

For MCI the slow-roll parameters and the number of e -foldings suffered from k_* can be calculated applying Eq. (2.8) and Eq. (2.7) – after removing hats and setting $J = 1$ – with results

$$\epsilon = \eta = 2/\bar{\sigma}^2 \quad \text{and} \quad N_* = (\bar{\sigma}_*^2 - \bar{\sigma}_f^2)/4. \quad (3.3)$$

Using these results, imposing the condition of Eq. (2.8) and employing Eq. (2.11) we can derive the following:

$$\bar{\sigma}_f = \sqrt{2}, \quad \bar{\sigma}_* \simeq 2\sqrt{N_*}, \quad n_s \simeq 1 - 2/N_* \quad \text{and} \quad r \simeq 8/N_*. \quad (3.4)$$

Clearly trans-Planckian values of σ are required and observationally favored n_s and r are obtained. More precisely, imposing the requirements (a) and (b) of Sec. 2.2 for several T_{rh} 's we get numerically the values of σ_* , m , n_s , α_s and r listed in Table 1 – c.f. Ref. [20]. As T_{rh} decreases, N_* decreases too – see Eq. (2.9) – and so, σ_* and n_s slightly decrease whereas r increases – see Eq. (3.4). The resulting n_s , α_s and r lie within the range of Eq. (2.10). In all cases, Eq. (2.12a) is valid whereas the upper bound of Eq. (2.12b) is surpassed.

3.2 RESULTS FOR NON-MCI

From Eqs. (3.3) and (3.4) we can infer that the amplitude of the inflaton field within non-MCI can become sub-Planckian if $J \gg 1$ and $\hat{V}_{,\sigma}/\hat{V} \simeq V_{,\sigma}/V$. These two objectives can be achieved if we employ $f(\sigma)$ given by Eq. (3.2) with $c_{\mathcal{R}} \gg 1$. Another possibility would be to take $f(\sigma) = \exp(-c_{\mathcal{R}}\bar{\sigma})$. However, in the latter case the resulting r violates Eq. (2.10c) and therefore, this option can be declined. Similar problem arises also if we increase the absolute value of the exponent in $f(\sigma)$.

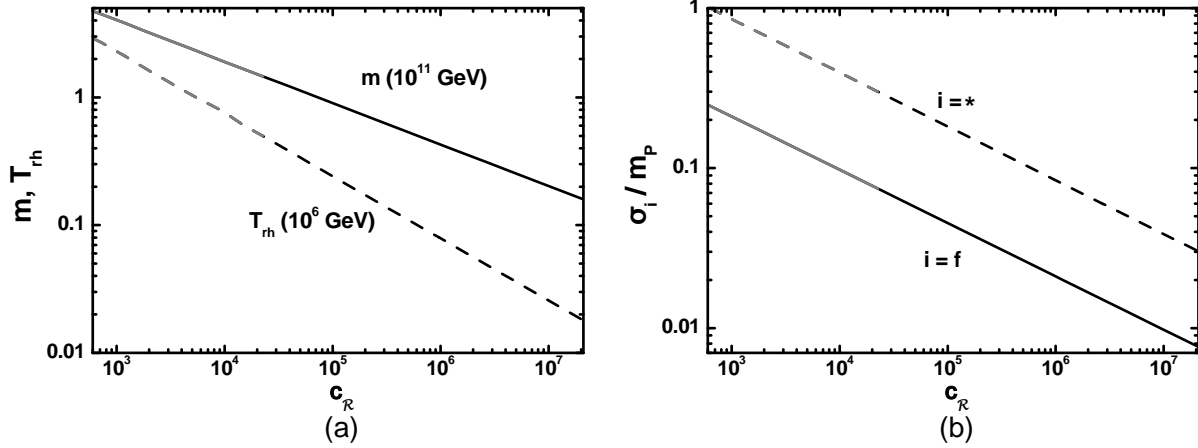


Figure 1: The allowed by Eqs. (2.5), (2.6), (2.7) and (2.9) values of m (solid line) and T_{rh} (dashed line) [σ_f (solid line) and σ_* (dashed line)] versus $c_{\mathcal{R}}$ for non-MCI (a) [(b)]. The gray segments denote values of the various quantities fulfilling Eq. (3.11) too.

Substituting Eq. (3.2) into Eqs. (2.3) and (2.5) and taking into account that $c_{\mathcal{R}} \gg 1$, we obtain

$$J \simeq \sqrt{c_{\mathcal{R}} \bar{\sigma}}, \quad \hat{V} = \frac{1}{2} m^2 \sigma^2 \left(1 + c_{\mathcal{R}} \frac{\sigma}{m_{\text{P}}} \right)^2 \simeq \frac{m^2 c_{\mathcal{R}}^2 \sigma^4}{2 m_{\text{P}}^2} \quad \text{and} \quad \Gamma_{\sigma} \simeq \frac{1}{192\pi} \frac{m_{\sigma}^3}{m_{\text{P}}^2} \quad (3.5)$$

where $m_{\sigma} = m$ and obviously $\langle \sigma \rangle = 0$. Upon use of Eqs. (2.8), (2.7) and (3.5), the slow roll parameters and \hat{N}_* read

$$(a) \quad \hat{\epsilon} \simeq \frac{8}{c_{\mathcal{R}} \bar{\sigma}^3}, \quad \hat{\eta} \simeq \frac{12}{c_{\mathcal{R}} \bar{\sigma}^3} = \frac{3}{2} \hat{\epsilon} \quad \text{and} \quad (b) \quad \hat{N}_* \simeq \frac{c_{\mathcal{R}}}{12} (\bar{\sigma}_*^3 - \bar{\sigma}_f^3). \quad (3.6)$$

Imposing the condition of Eq. (2.8) and solving then Eq. (3.6b) w.r.t σ_* we arrive at

$$\bar{\sigma}_f \simeq (12/c_{\mathcal{R}})^{1/3} \quad \text{and} \quad \bar{\sigma}_* \simeq \left(12 \hat{N}_* / c_{\mathcal{R}} \right)^{1/3}. \quad (3.7)$$

Inserting the last results into Eq. (3.6a), we find through Eq. (2.11)

$$(a) \quad n_s \simeq 1 - 3\hat{\epsilon}_* = 1 - 2/\hat{N}_* \simeq (0.952 - 0.955) \quad \text{and} \quad (b) \quad r \simeq 32/3\hat{N}_* \simeq (0.2 - 0.22), \quad (3.8)$$

where the ranges above are derived numerically letting $c_{\mathcal{R}}$ vary within its allowed region – see below. Notice that the resulting n_s 's are a little lower than those listed in Table 1 whereas r is significantly elevated and can be probed in the near future from the measurements of PLANCK satellite [34]. Note, in passing, that the so-called Lyth bound [35] on the σ variation, $\Delta\sigma$, gets modified within non-MI. Namely, combining Eqs. (2.7) and (2.8) we find

$$\frac{d\sigma}{d\hat{N}} = \sqrt{\frac{r}{8}} \frac{m_{\text{P}}}{J} \Rightarrow \Delta\sigma = \sqrt{\frac{r}{8}} \frac{m_{\text{P}}}{J} \Delta\hat{N} \Rightarrow \Delta\sigma \gtrsim \sqrt{2r} \frac{m_{\text{P}}}{J} \simeq (2.5 - 0.083) m_{\text{P}}/100, \quad (3.9)$$

taking [35] $\Delta\hat{N} \simeq \Delta N = 4$ and assuming negligible variation of f from its value at $\sigma = \sigma_*$. Therefore, large r 's do not correlate necessarily with trans-Planckian $\Delta\sigma$'s within non-MI.

In our numerical code we use as input parameters m , σ_* and $c_{\mathcal{R}}$. For every chosen $c_{\mathcal{R}}$ we restrict m and σ_* so as the conditions (a) and (b) of Sec. 2.2 – with T_{rh} evaluated consistently with Eq. (2.5) – are fulfilled. Our results are presented in Fig. 1 where we draw the allowed values of m (solid line) and T_{rh} (dashed line) [σ_f (solid line) and σ_* (dashed line)] versus $c_{\mathcal{R}}$ for non-MCI (a) [(b)]. Satisfaction of

Eq. (2.12b) gives a lower bound on $c_{\mathcal{R}}$ – see Fig. 1-(b) –, whereas Eq. (2.10c) provides an upper bound on $c_{\mathcal{R}}$. This depends, though very weakly, on \hat{N}_{tot} and therefore, on the reheating mechanism – see Eq. (3.8b) and Eq. (2.9). From our data we also remark that the resulting m 's [α_s 's] are almost two orders [one order] of magnitude lower than those obtained within MCI. All in all, we obtain

$$625 \lesssim c_{\mathcal{R}} \lesssim 2.1 \cdot 10^7, \quad 47 \gtrsim \frac{m}{10^7 \text{ TeV}} \gtrsim 1.6, \quad 52 \gtrsim \hat{N}_* \gtrsim 47.9, \quad \text{and} \quad 8.5 \lesssim \frac{\alpha_s}{0.001} \lesssim 9.9. \quad (3.10)$$

As for SM non-MI [2–4], in our proposal there is a coupling constant, $c_{\mathcal{R}}$, which takes unusually large values. Following the arguments of Ref. [6–8] we below comment on the naturalness of our model. Indeed, the used $c_{\mathcal{R}}$'s could jeopardize the validity of the classical approximation, on which the analysis of the inflationary behavior in Sec. 2.2 is based. The resulting \hat{V} in Eq. (3.5) is non-renormalizable and suggests that the theory breaks down for energies of the order $\Lambda = m_{\text{P}}/c_{\mathcal{R}}$. Therefore, consistency with the validity of the effective theory implies that the inflationary scale – represented by the Hubble parameter at horizon crossing in the Einstein frame, $\hat{H}_* = \hat{V}(\sigma_*)^{1/2}/\sqrt{3}m_{\text{P}}$ – is to be lower than Λ , i.e., $\hat{H}_* \ll \Lambda$. Numerically we find

$$0.03 \lesssim \hat{H}_*/\Lambda \lesssim 1 \quad \text{for} \quad 625 \lesssim c_{\mathcal{R}} \lesssim 2.26 \cdot 10^4 \quad \text{and} \quad 1 \gtrsim \bar{\sigma}_* \gtrsim 0.3, \quad (3.11)$$

where the corresponding ranges of values are depicted by the gray segments of the lines in Fig. 1. The range in Eq. (4.1) turns out to be a little more comfortable than the one we get within SM non-MI – c.f. Ref. [6].

On the other hand, non-renormalizable terms in \mathcal{S} suggest that the cutoff scale of the effective theory is equal to m_{P} . In fact, such terms arise from the the first term in Eq. (2.1) and the second one in Eq. (2.3). In our model, the form of these terms is generated expanding the relevant coefficients in series around $\sigma = \sigma_*$ with the following result – an expansion in the small field limit, $c_{\mathcal{R}}\sigma \ll 1$, fails to reproduce the exact results:

$$m_{\text{P}}^2 f_{\mathcal{R}} \ni \frac{1}{c_{\mathcal{R}}\bar{\sigma}_*} \left(1 - 3\frac{\bar{\sigma}}{\bar{\sigma}_*} + 10\left(\frac{\bar{\sigma}}{\bar{\sigma}_*}\right)^2 + \dots \right) \partial^{\bar{\mu}}\partial_{\bar{\mu}}h^{\mu\nu} \quad (3.12a)$$

$$\text{and} \quad m_{\text{P}}^2 \frac{f_{,\sigma}}{f^2} \hat{g}^{\mu\nu} \partial_{\mu}\sigma\partial_{\nu}\sigma \ni \frac{1}{\bar{\sigma}_*^2} \left(1 - 8\frac{\bar{\sigma}}{\bar{\sigma}_*} + 45\left(\frac{\bar{\sigma}}{\bar{\sigma}_*}\right)^2 + \dots \right) \hat{g}^{\mu\nu} \partial_{\mu}\sigma\partial_{\nu}\sigma, \quad (3.12b)$$

where $h^{\mu\nu}$ denotes the graviton field involved in the expansion [6,7] of the metric $g^{\mu\nu} \simeq \eta^{\mu\nu} + h^{\mu\nu}/m_{\text{P}}$ around the Minkowski space with metric $\eta^{\mu\nu}$ and \mathcal{R} is approximated linearly. In agreement with the argument above, perturbative calculation of the $\sigma\sigma$ cross section through the interactions in Eq. (3.12a) seem to indicate [8] that the effective cutoff is equal to m_{P} . Given these ambiguities, we do not consider the condition $\hat{H}_* \ll \Lambda$ as an absolute constraint.

Let us finally emphasize that, in contrast to the models suggested in Ref. [20], \hat{V} remains concave upwards in our scheme. Therefore, non-MCI is not of hilltop type and so, complications related to the initial conditions are avoided. As we explicitly checked, possible inclusion of extra radiative corrections in Eq. (3.1) due to a coupling of σ to fermions – considered in Ref. [20] – do not affect our proposal for values of the relevant Yukawa coupling constant, h , lower than about 10^{-3} . For such h 's, the decay width of the inflaton due to this channel dominates over the one given by Eq. (2.5).

4 NON-MINIMAL HYBRID INFLATION

HI is realized in the presence of two real scalar fields, σ and ϕ , involved in the following potential [11]

$$V(\phi, \sigma) = \kappa^2 \left(M^2 - \frac{\phi^2}{4} \right)^2 + \frac{m^2\sigma^2}{2} + \frac{\lambda^2\phi^2\sigma^2}{4}, \quad (4.1)$$

where M, m are mass parameters and κ, λ are dimensionless coupling constants. The global minima of V lie at $(\langle\sigma\rangle, \langle\phi\rangle) = (0, \pm 2M)$. Therefore, V leads to a spontaneous symmetry breaking of a global or local symmetry depending on the nature of the waterfall field ϕ . In the latter case, topological defects may be also produced via the Kibble mechanism [36]. Trying to keep our approach as simple as possible we below assume that this is not the case.

In addition, V in Eq. (4.1) gives rise to HI. This is because V possesses an almost σ -flat direction at $\phi = 0$ with constant potential density equal to $V_0 = V(\phi = 0, \sigma) = \kappa^2 M^4$, for $m = 0$. The effective mass squared of the field ϕ along this direction is

$$m_\phi^2 = -\kappa^2 M^2 + \lambda^2 \sigma^2 / 2 > 0 \Leftrightarrow \sigma > \sigma_c = \sqrt{2} \kappa M / \lambda. \quad (4.2)$$

Thus, for $\sigma > \sigma_c$ the $\phi = 0$ direction represents a valley of minima which can serve as inflationary trajectory. On this path the potential of HI takes the form

$$V = V_0 + \frac{1}{2} m^2 \sigma^2 + V_{\text{rc}} \quad (4.3)$$

where V_{rc} is the one-loop correction (to the tree level potential) which can be written as [21, 23]

$$V_{\text{rc}} = \frac{1}{64\pi^2} \left(m^4 \ln \frac{m^2}{Q^2} + \kappa^2 V_0 (x-1)^2 \ln \frac{\kappa^2 M^2}{Q^2} (x-1) \right) \text{ with } x = \left(\frac{\sigma}{\sigma_c} \right)^2 \quad (4.4a)$$

$$\simeq \frac{\kappa^2 V_0}{64\pi^2} \left(x^2 \ln \frac{\kappa^2 M^2}{Q^2} + \frac{3}{2} \right) \text{ for } x \gg 1. \quad (4.4b)$$

Here, Q is a renormalization scale which can be conveniently chosen [21] equal to σ_c which practically coincides with the value of σ at the end of HI, σ_f .

We below review (Sec. 4.1) the results for MHI (with $f(\sigma) = 1$) and describe (Sec. 4.2) our findings for non-MHI, seeking the following non-minimal coupling function for the inflaton – for earlier attempts on non-MHI, see Ref. [37]:

$$f(\sigma) = 1 - c_{\mathcal{R}} \bar{\sigma} / (1 + \bar{\sigma})^2 \quad (4.5)$$

where we use, as usual, the shorthand $\bar{\sigma} = \sigma / m_{\text{P}}$. As regards the waterfall field we can assume that it is either minimally coupled to gravity or its coupling function is $f(\phi)$ since $f(0) = 1$ and $f(2M) \simeq 1$ for $c_{\mathcal{R}} \ll 1$ and $M \leq m_{\text{P}}$.

4.1 RESULTS FOR MHI

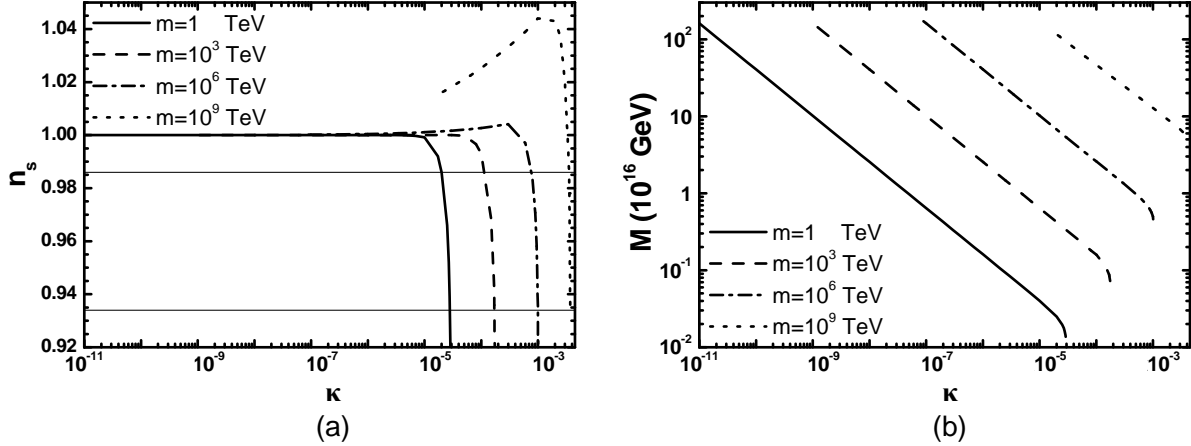
We can get an impression of the expected results for MHI, if we calculate the, involved in the inflationary dynamics, derivatives of V in Eq. (4.3). Namely we have

$$V_{,\sigma} = m^2 \sigma + \frac{x \kappa^2 V_0}{32\pi^2 \sigma} (x-1) \left(2 \ln \frac{\kappa^2 M^2}{Q^2} (x-1) + 1 \right). \quad (4.6)$$

We observe that there are two contributions in $V_{,\sigma}$. The first one arises from the tree-level potential whereas the second one comes from the radiative corrections in Eq. (4.4a). When the first contribution dominates over the second one, we obtain the well-known tree-level [11] results, $N_{\text{tr}*}$ and η_{tr} , for N_* and η respectively:

$$N_{\text{tr}*} = \frac{1}{\eta_{\text{tr}}} \ln \frac{\sigma_*}{\sigma_c} \text{ with } \eta_{\text{tr}} = m_{\text{P}}^2 \frac{m^2}{V_0} \gg \epsilon. \quad (4.7)$$

In this regime, the resulting n_s clearly – see Eq. (2.11) – exceeds slightly unity in contrast to the observationally favored results of Eq. (2.10a). Moreover, as we find numerically, the lower κ and/or m we use, the closer σ_* is set to σ_c . This is the first kind of tuning occurred within MHI.



m (TeV)	κ (10^{-3})	M (10^{16} GeV)	Δ_{c*}	Δ_{m*}
1	0.02 – 0.028	0.025 – 0.015	0.00016 – 0.00029	0.0004 – 0.00007
10^3	0.12 – 0.17	0.13 – 0.083	0.0053 – 0.01	0.013 – 0.0023
10^6	0.8 – 1	0.69 – 0.49	0.18 – 0.31	0.19 – 0.054
10^9	3.55 – 3.72	5.98 – 5.5	4.4 – 5.7	0.38 – 0.24

Figure 2: The allowed by Eqs. (2.6), (2.7) and (2.9) values of n_s (a) and M (b) versus κ for MHI with $T_{\text{rh}} = 10^{10}$ GeV, $\kappa = \lambda$ and several m 's indicated in the graphs. Shown are also in table the allowed ranges of the various parameters for n_s in the range of Eq. (2.10a) limited by thin lines (a).

Nonetheless, taking into account that the logarithm in Eq. (4.6) turns out to be negative, we can show that, for every m , there is κ such that V develops a maximum at $\sigma = \sigma_{\text{max}}$, which can be estimated by numerically solving the condition $V_{,\sigma}(\sigma_{\text{max}}) = 0$. At $\sigma = \sigma_{\text{max}}$, $V_{,\sigma\sigma}$ given by

$$V_{,\sigma\sigma} = \frac{V_{,\sigma}}{\sigma} + \frac{x^2 \kappa^2 V_0}{16\pi^2 \sigma^2} \left(2 \ln \frac{\kappa^2 M^2}{Q^2} (x-1) + 3 \right), \quad (4.8)$$

becomes negative and so, η and n_s start decreasing for σ_* close σ_{max} – see Eqs. (2.8) and (2.11). As for any model of hilltop inflation, the lower n_s we obtain, the closer σ_* is located to σ_{max} . This is a second kind of tuning which remains even for non-MHI – see Sec. 4.2. To quantify somehow the amount of the tunings encountered in the considered model, we define the quantities:

$$(a) \Delta_{m*} = \frac{\sigma_{\text{max}} - \sigma_*}{\sigma_{\text{max}}} \quad \text{and} \quad (b) \Delta_{c*} = \frac{\sigma_* - \sigma_c}{\sigma_c}. \quad (4.9)$$

The above rough estimations can be verified by our numerical computations. In our code, we use as input parameters κ , λ , m , M , σ_* and T_{rh} . In our analysis for MHI, we fix $T_{\text{rh}} = 10^{10}$ GeV and $\kappa = \lambda$ – possible variation of these two choices do not modify our conclusions in any essential way. For any chosen κ and m we then restrict M and σ_* so as the restrictions (a), (b) and (d) of Sec. 2.2 are fulfilled. Using Eq. (2.11) we can extract n_s and α_s . Our results are presented in Fig. 2-(a) [Fig. 2-(b)] where we design the allowed values of n_s [M] versus κ for $m = 1$ TeV (solid line) or $m = 10^3$ TeV (dashed line) or $m = 10^6$ TeV (dot-dashed line) or $m = 10^9$ TeV (dotted line). The region of Eq. (2.10a) is also limited by thin lines. The various lines terminate at low κ 's due to the saturation of Eq. (2.12b) and at large κ 's since the satisfaction of the imposed conditions can not be achieved.

Clearly, the almost horizontal part of the various lines, which exceeds the observational limits of Eq. (2.10a), in the $\kappa - n_s$ plane corresponds to the dominance of the tree level potential. However, for

any m and relatively large κ 's we can obtain acceptable n_s 's even without inclusion of extra radiative corrections due to a possible coupling of the inflaton to fermions – c.f. Ref. [21]. On the other hand, it is worth emphasizing that the allowed range of κ 's for each m is severely tuned. Indeed, confining n_s within the range of Eq. (2.10a) we find the ranges of the parameters listed in the table of Fig. 2. From the outputs there, we also remark that κ 's, M 's, Δ_{c^*} 's and Δ_{m^*} 's increase with m . Therefore, the natural realization of MHI requires large m 's. In this case too, M turns out to be well above its value within the SUSY version HI – c.f. Ref. [15, 16]. Needless to say, finally, that the resulting α_s 's and r 's turn out to be vanishingly small and so, uninteresting. In conclusion, MHI (with the minimal possible radiative corrections) is rather disfavored by the current observational data.

4.2 RESULTS FOR NON-MHI

From the analysis of MHI we can deduce that reduction of n_s for a wider range of κ 's can be achieved if the slope of V becomes less steep. This objective can be achieved if we employ $f(\sigma)$ given by Eq. (4.5) with $c_{\mathcal{R}} \ll 1$. Another possibility would be $f(\sigma) = \exp(-c_{\mathcal{R}}\bar{\sigma})$. However, in the latter case the resulting σ_* violates the bound of Eq. (2.12b) and therefore, the latter option is not adoptable.

Differentiating Eq. (4.5) w.r.t σ , substituting into Eqs. (2.3) and (2.5) and taking into account that $c_{\mathcal{R}} \ll 1$, we obtain

$$f_{,\sigma} = \frac{c_{\mathcal{R}}(-1 + \bar{\sigma})}{m_{\text{P}}(1 + \bar{\sigma})^3}, \quad f_{,\sigma\sigma} = \frac{2c_{\mathcal{R}}(2 - \bar{\sigma})}{m_{\text{P}}^2(1 + \bar{\sigma})^4}, \quad \hat{V} \simeq V_0, \quad J \simeq 1 \quad \text{and} \quad \Gamma_{\sigma} = \frac{c_{\mathcal{R}}^2 m_{\sigma}^3}{128\pi m_{\text{P}}^2} \quad (4.10)$$

where $m_{\sigma} = \sqrt{2\lambda^2 M^2 + m^2}$. Despite the fact that \hat{V} given by Eqs. (2.3) and (4.3) is practically equal to V_0 – since $f(\bar{\sigma}) \simeq 1$ for $\bar{\sigma} \ll 1$ –, its inclination is mostly dominated by the term $-2V_0 f_{,\sigma}$ of $V_{,\sigma}$. Indeed, upon use of Eqs. (2.8), (4.4b) and (4.10) we find

$$\hat{\epsilon} = \frac{m_{\text{P}}^2}{2} \left(-2f_{,\sigma} + \frac{m^2\sigma}{V_0} + \frac{\kappa^2 x^2}{16\pi^2 \sigma} \ln \frac{\kappa^2 M^2}{Q^2} \right)^2. \quad (4.11)$$

In a sizable portion of the parameter space, the first contribution to $\hat{\epsilon}$ in Eq. (4.11) overshadows the others two. As a consequence, \hat{V} develops a maximum at $\bar{\sigma} = \bar{\sigma}_{\text{max}}$ for $f_{,\sigma}(\bar{\sigma}_{\text{max}}) = 0 \Leftrightarrow \bar{\sigma}_{\text{max}} \simeq 1$ with $\hat{V}_{,\sigma\sigma}(\sigma_{\text{max}}) < 0$. In fact, inserting Eqs. (2.3) and (4.3) into Eq. (2.8) we end up with

$$\hat{\eta} = m_{\text{P}}^2 \left(-2f_{,\sigma\sigma} + \frac{m^2}{V_0} + \frac{3\kappa^2 x^2}{16\pi^2 \sigma^2} \ln \frac{\kappa^2 M^2}{Q^2} \right), \quad (4.12)$$

which is negative for dominant $f_{,\sigma\sigma}$ with $\bar{\sigma} < 2$. Combining Eqs. (4.12) with (2.11a) we can easily infer that $c_{\mathcal{R}} > 0$ for $\bar{\sigma} < \bar{\sigma}_{\text{max}}$ strengthens significantly the reduction of n_s . Neglecting the two last terms in the right-hand side of Eq. (4.11), we can estimate \hat{N}_* via Eq. (2.7) with result

$$\hat{N}_* \simeq \frac{1}{2m_{\text{P}}^2} \int_{\sigma_*}^{\sigma_c} \frac{d\sigma}{f_{,\sigma}} = \frac{1}{6c_{\mathcal{R}}} \left((21 + 6\bar{\sigma}_* + \bar{\sigma}_*^2) \bar{\sigma}_* - (21 + 6\bar{\sigma}_c + \bar{\sigma}_c^2) \bar{\sigma}_c + 24 \ln \frac{1 - \bar{\sigma}_*}{1 - \bar{\sigma}_c} \right). \quad (4.13)$$

As we verify numerically, the formula above gives accurate results for $m \leq 10^6$ TeV and sufficiently low κ 's. However, since σ_* depends on \hat{N}_* in a rather complicate way, it is not doable to find an analytical result for n_s as a function of \hat{N}_* – c.f. Eq. (3.7). Therefore, our last resort is the numerical computation, whose the results are presented in the following.

In our code, we use as input parameters κ , λ , m , M , σ_* and $c_{\mathcal{R}}$. Note that T_{rh} is calculated via Eq. (2.5). For every chosen κ , λ , m and $c_{\mathcal{R}}$, we can restrict M and σ_* so as the conditions (a), (b) and (d) of Sec. 2.2 are fulfilled. Through Eq. (2.11) we can then extract n_s and α_s . Following this strategy, in Fig. 4-(a) [Fig. 4-(b)] we display the allowed values of n_s [M] versus $c_{\mathcal{R}}$ with $m \leq 10^6$ TeV,

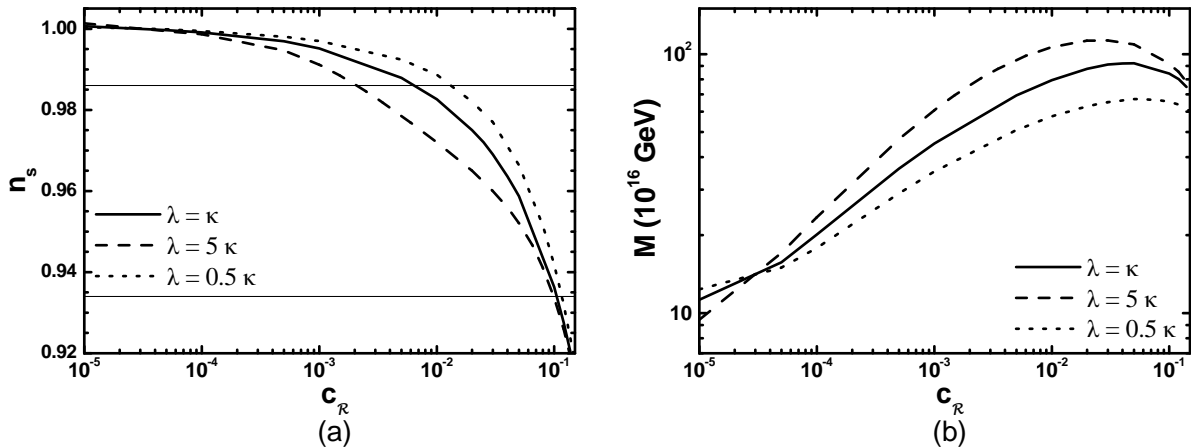


Figure 3: The allowed by Eqs. (2.6), (2.7) and (2.9) – with T_{rh} given by Eq. (2.5) – values of n_s (a) and M (b) versus $c_{\mathcal{R}}$ for non-MHI with $m \leq 10^6$ TeV, $\kappa = 10^{-5}$ and several λ 's indicated in the graphs. The region of Eq. (2.10a) is also limited by thin lines.

$\kappa = 10^{-5}$ and $\lambda = \kappa$ (solid lines) $\lambda = 5\kappa$ (dashed lines) and $\lambda = 0.5\kappa$ (dotted lines). The region of Eq. (2.10a) is also limited by thin lines. We observe that as $c_{\mathcal{R}}$ increases, n_s decreases entering the observationally favored region of Eq. (2.10a). On the other hand, M increases with $c_{\mathcal{R}}$ until a certain $c_{\mathcal{R}} \simeq 0.03 - 0.05$ and then decreases. Surprisingly the value of $c_{\mathcal{R}}$, at which the maximum M is encountered, corresponds more or less to the central observational $n_s \simeq 0.96$. We also observe that increasing λ above κ with fixed $c_{\mathcal{R}}$, n_s drops but M raises. These results can be understood as follows: As λ/κ elevates σ_c decreases – see Eq. (4.2) – and therefore, σ_* decreases, with fixed \hat{N}_* . This effect causes an increase of $|f_{,\sigma}(\sigma_*)|$ and $f_{,\sigma\sigma}(\sigma_*)$ – see Eq. (4.10). As a consequence, M increases too, since M is proportional to $f_{,\sigma}^{1/2}$ due to Eq. (2.6). Also, $|\eta|$ increases – according to Eq. (4.12) – and so, n_s drops efficiently – see Eq. (2.11).

Confronting non-MHI with all the constraints of Sec. 2.2, we can delineate the allowed (lightly gray shaded) regions in the $\kappa - c_{\mathcal{R}}$ [$\kappa - M$] plane as in Fig. 4-(a₁), (b₁) and (c₁) [Fig. 4-(a₂), (b₂) and (c₂)]. In Fig. 4-(a₁) and (a₂) we take $\lambda = \kappa$. Our results for this choice are m -independent for any κ and $m \leq 10^6$ TeV. On the other hand, in Fig. 4-(b₁) and (b₂) [Fig. 4-(c₁) and (c₂)] we set $\lambda = 5\kappa$ and $m = 10^8$ TeV and [$\lambda = 0.5\kappa$ and $m = 10^7$ TeV]. The conventions adopted for the various lines are also shown in the left-hand side of each graph. In particular, the gray dot-dashed [dashed] lines correspond to $n_s = 0.986$ [$n_s = 0.934$], whereas the gray solid lines have been obtained by fixing $n_s = 0.96$ – see Eq. (2.10). For κ 's below the solid black line, our initial requirement in Eq. (2.12b) is violated. For κ 's larger than those depicted in the graphs we do not find solutions consistent with the imposed restrictions of Sec. 2.2. The upper bounds of the allowed regions in the $\kappa - M$ plane come from $c_{\mathcal{R}}$ leading to $n_s = 0.96$. Although this result is not precisely exact, it is accurate enough for our pictorial purposes. In all cases, the allowed ranges of κ 's – although restricted to values lower than 0.001 – are much more wide and natural than the ones obtained for MHI – c.f. Table of Fig. 2. Confining n_s to its central observational value, we obtain the ranges of the various parameters arranged in the Table of Fig. 4. We observe there that, for fixed n_s and increasing κ , $c_{\mathcal{R}}$ and M decrease whereas Δ_{c^*} and Δ_{m^*} increase. As a consequence, for any m , the tuning regarding Δ_{c^*} is greatly alleviated compared to the outputs of MHI, whereas we are let with the usual mild tuning required for Δ_{m^*} . This is present to any inflationary hilltop model – c.f. Ref. [16]. The allowed M 's mostly exceed the SUSY grand unification scale, $M_{\text{GUT}} \simeq 2.86 \cdot 10^{16}$ GeV, whereas T_{rh} mostly increases with κ , as can be noticed via Eqs. (2.5) and (4.10).

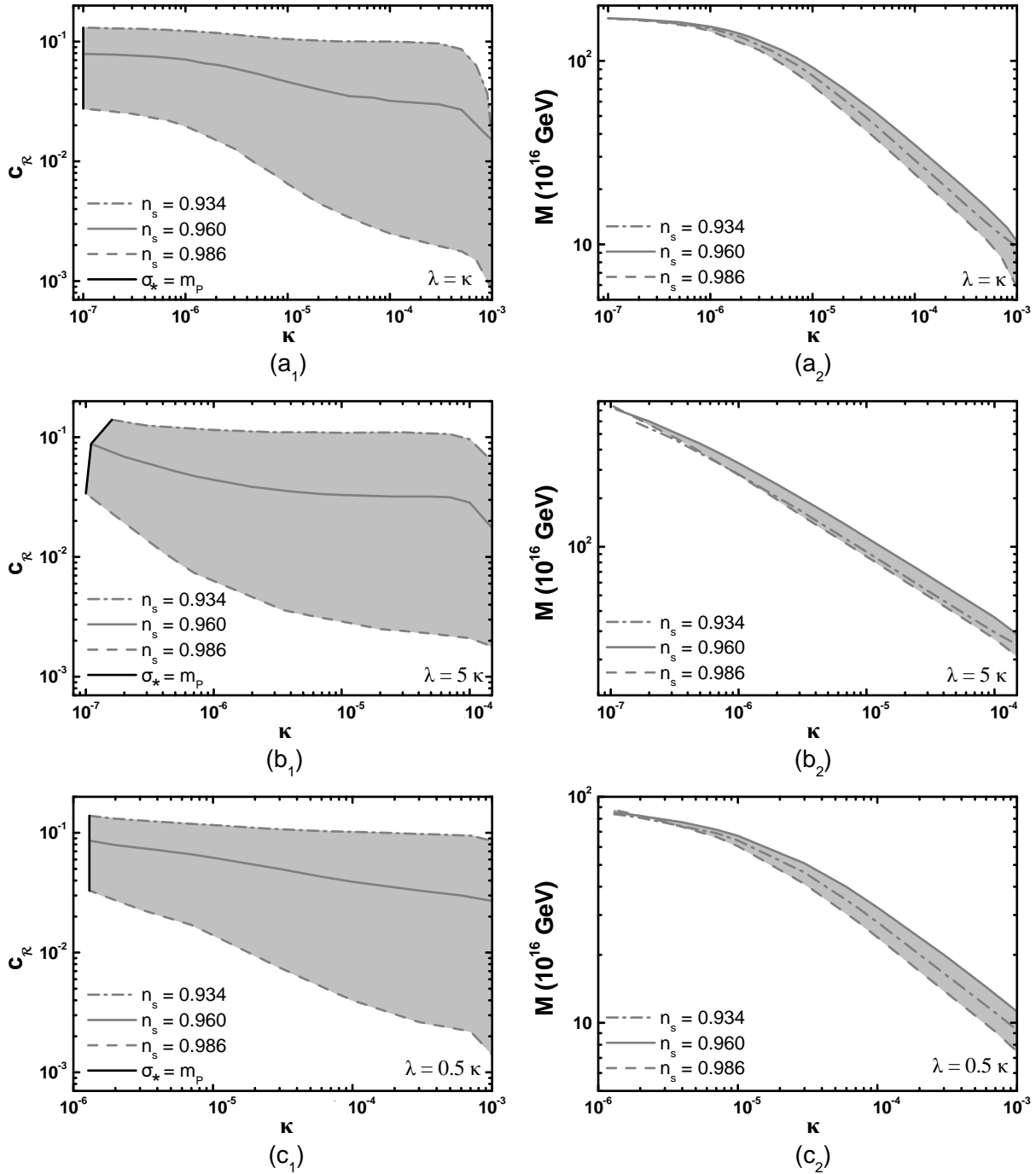


Fig.	$\kappa/10^{-3}$	$c_{\mathcal{R}}/10^{-2}$	$M/10^{16}$ GeV	$T_{\text{rh}}/10^8$ GeV	Δ_{c^*}	$\Delta_{m^*}/10^{-2}$
(a ₁), (a ₂)	0.0002 – 1	7.8 – 1.5	168 – 10	0.0028 – 3.5	0.016 – 7	0.91 – 31
(b ₁), (b ₂)	0.00011 – 0.2	8.8 – 1.8	711 – 25	0.12 – 13	0.21 – 18	9.6 – 32
(c ₁), (c ₂)	0.0013 – 1	8.6 – 2.7	85 – 11	0.006 – 2.1	0.03 – 4	1.5 – 32

Figure 4: Allowed (lightly gray shaded) by the restrictions of Sec. 2.2 areas in the $\kappa - c_{\mathcal{R}}$ [$\kappa - M$] plane (a₁, b₁ and c₁) [(a₂ b₂ and c₂)] for non-MHI. We take $\kappa = \lambda$ and $m \leq 10^6$ TeV (a₁ and a₂) or $m = 10^8$ TeV and $\lambda = 5\kappa$ (b₁ and b₂) or $m = 10^7$ TeV and $\lambda = 0.5\kappa$ (c₁ and c₂). The conventions adopted for the various lines are also shown. The allowed ranges of the various parameters for $n_s = 0.96$ are listed in the table.

From our findings, we can conclude that: (i) the required $c_{\mathcal{R}}$'s are rather low and so, complications related to the hierarchy between the inflationary scale and the effective cutoff of the theory are avoided; (ii) our results depend rather weakly on the variation of m , for $m \leq 5 \cdot 10^8$ TeV; (iii) as m 's raise above $5 \cdot 10^8$ TeV and κ drops below 0.001, Eq. (2.12b) is eventually violated and so, our scheme is not applicable; (iv) similarly to MHI, α_s and r turn out to be negligibly small.

As in the case of non-MCI, our proposal remains intact even if we add fermion-dominated one-loop radiative corrections in Eq. (4.3) – c.f. Ref. [21] – provided the values of the relevant Yukawa coupling constant, h , remains lower than about 10^{-4} . For h 's close to this value, the decay width of the inflaton, due to this channel dominates over the one given by Eq. (2.5).

5 CONCLUSIONS

We considered the non-SUSY version of CI (driven by quadratic potential) and HI, assuming a non-minimal coupling function, $f(\sigma)$, between the inflaton field and the Ricci scalar curvature. Using the freedom of choosing this scalar function, we deliberated CI from the problem of trans-Planckian inflaton values and achieved observationally acceptable n_s 's for a wide range of the parameters of HI. As a bonus, the selected $f(\sigma)$'s give rise to Yukawa-type interactions between the inflaton and matter fields leading to a successful post-inflationary reheating. Afterwards, the proposed $f(\sigma)$'s reduce to unity and so, Einstein gravity is naturally recovered.

Specifically, the adopted forms of $f(\sigma)$ are given by Eq. (3.2) and Eq. (4.5) for non-MCI and non-MHI, respectively. In both cases, the parameter $c_{\mathcal{R}}$ involved in $f(\sigma)$ can be constrained so as the results of the inflationary models can be reconciled with a number of theoretical and observational restrictions. In the case of non-MCI, we find $625 \lesssim c_{\mathcal{R}} \lesssim 2.1 \cdot 10^7$ resulting to $n_s \simeq 0.955$ and tensor-to-scalar ratio $r \simeq (0.2 - 0.22)$. In sharp contrast to MCI, only sub-Planckian values of the inflaton field are utilized. Comments on the naturalness of the model are also given. In the case of non-MHI, the chosen $f(\sigma)$ leads to hilltop-type inflation for a wide range for κ 's. As a consequence, observationally acceptable results require a proximity between the values of the inflaton field at the maximum of the potential and at the horizon crossing of the pivot scale. The amount of this tuning was measured by the quantity Δ_{m*} defined in Eq. (4.9b). E.g., for $m \leq 10^6$ TeV and the observationally central value of n_s , we find $c_{\mathcal{R}} \simeq (0.015 - 0.078)$ with $M \simeq (1 - 16.8) \cdot 10^{17}$ GeV, $\lambda = \kappa \simeq (2 \cdot 10^{-7} - 0.001)$ and $\Delta_{m*} \simeq (0.91 - 32)\%$. Compared to MHI, we find that satisfaction of the observational requirements can be achieved without tuning severely neither κ nor Δ_{c*} defined in Eq. (4.9a) even for low m 's (see Tables of Figs. 2 and 4). Therefore, the proposed non-MHI is more favored by the current data.

We checked explicitly that for both models of non-MI the proposed scheme remains valid even if extra coupling of the inflaton to fermions exists, provided that the relevant coupling constant is somewhat suppressed. If these fermions are identified with right-handed neutrinos, baryogenesis via non-thermal leptogenesis [38] is, in principle, possible. Note that, in our framework, decay of the inflaton to right-handed neutrinos is also possible due to curvature-induced [24] couplings. However, the resulting decay widths are reduced [24] compared to those of the inflaton to bosons. As a consequence, the branching ratio of the inflaton's decay width to right-handed neutrinos is diminished and so, the produced lepton asymmetry is lower than the expectations for all possible masses of right-handed neutrinos. On the other hand, since baryogenesis can be realized in a variety of ways – see, e.g., Ref. [25, 39] – we opted not to complicate our presentation with secondary mechanisms which may or may not affect the inflationary observable quantities.

It would be interesting to investigate if a similar realization of non-MI can be accomplished in the framework of SUGRA, along the lines of Ref. [40]. In such a case, the inflaton of non-MCI could be identified with one of the right-handed sneutrinos. On the other hand, a possible SUSY version [15, 16] of non-MHI could become compatible with larger (and more natural) values of the relevant coupling constant $\kappa = \lambda$.

REFERENCES

- [1] K. Nozari and S.D. Sadatian, *Mod. Phys. Lett.* **A23**, 2933 (2008) [arXiv:0710.0058].
- [2] F.L. Bezrukov and M. Shaposhnikov, *Phys. Lett. B* **659**, 703 (2008) [arXiv:0710.3755];
A.O. Barvinsky *et al.*, *J. Cosmol. Astropart. Phys.* **11**, 021 (2008) [arXiv:0809.2104];
N. Okada, M. Ur Rehman and Q. Shafi, arXiv:0911.5073.
- [3] S.C. Park and S. Yamaguchi, *J. Cosmol. Astropart. Phys.* **08**, 009 (2008) [arXiv:0801.1722].
- [4] A. De Simone, M.P. Hertzberg and F. Wilczek, *Phys. Lett. B* **678**, 1 (2009) [arXiv:0812.4946].
- [5] T.E. Clark, B. Liu, S.T. Love and T. ter Veldhuis, *Phys. Rev. D* **80**, 075019 (2009) [arXiv:0906.5595];
R.N. Lerner and J. McDonald, *Phys. Rev. D* **80**, 123507 (2009) [arXiv:0909.0520].
- [6] C.P. Burgess, H.M. Lee and M. Trott, *J. High Energy Phys.* **09**, 103 (2009) [arXiv:0902.4465];
J.L.F. Barbon and J.R. Espinosa, *Phys. Rev. D* **79**, 081302 (2009) [arXiv:0903.0355];
C.P. Burgess, H.M. Lee and M. Trott, arXiv:1002.2730.
- [7] R.N. Lerner and J. McDonald, arXiv:0912.5463.
- [8] M.P. Hertzberg, arXiv:1002.2995;
S.R. Huggins and D.J. Toms, *Class. Quant. Grav.* **4**, 1509 (1987).
- [9] D.H. Lyth and A. Riotto, *Phys. Rept.* **314**, 1 (1999) [hep-ph/9807278];
A. Mazumdar and J. Rocher, arXiv:1001.0993.
- [10] A.D. Linde, *Phys. Lett. B* **129**, 177 (1983).
- [11] A.D. Linde, *Phys. Rev. D* **49**, 748 (1994);
E.J. Copeland *et al.*, *Phys. Rev. D* **49**, 6410 (1994) [astro-ph/9401011].
- [12] E. Komatsu *et al.* [WMAP Collaboration], *Astrophys. J. Suppl.* **180**, 330 (2009) [arXiv:0803.0547];
E. Komatsu *et al.* [WMAP Collaboration], arXiv:1001.4538
<http://lambda.gsfc.nasa.gov/product/map/dr2/parameters.cfm>
- [13] S. Clesse and J. Rocher, *Phys. Rev. D* **79**, 103507 (2009) [arXiv:0809.4355].
- [14] M. Kawasaki, M. Yamaguchi and T. Yanagida, *Phys. Rev. Lett.* **85**, 3572 (2000) [hep-ph/0004243];
M.C. Bento, R.G. Felipe and N.M.C. Santos, *Phys. Rev. D* **69**, 123513 (2004) [hep-ph/0402276];
M. Bastero-Gil and A. Berera, *Phys. Rev. D* **71**, 063515 (2005) [hep-ph/0507124];
S. Dimopoulos *et al.*, *J. Cosmol. Astropart. Phys.* **08**, 003 (2008) [hep-th/0507205].
- [15] G.R. Dvali, Q. Shafi and R.K. Schaefer, *Phys. Rev. Lett.* **73**, 1886 (1994) [hep-ph/9406319].
- [16] M. Bastero-Gil, S.F. King and Q. Shafi, *Phys. Lett. B* **651**, 345 (2007) [hep-ph/0604198];
B. Garbrecht, C. Pallis and A. Pilaftsis, *J. High Energy Phys.* **12**, 038 (2006) [hep-ph/0605264];
M. Ur Rehman, V.N. Şenoğuz and Q. Shafi, *Phys. Rev. D* **75**, 043522 (2007) [hep-ph/0612023];
C. Pallis, *J. Cosmol. Astropart. Phys.* **04**, 024 (2009) [arXiv:0902.0334];
M. Ur Rehman, Q. Shafi and J.R. Wickman, *Phys. Lett. B* **683**, 191 (2010) [arXiv:0908.3896];
M. Ur Rehman, Q. Shafi and J.R. Wickman, arXiv:0912.4737.
- [17] R.A. Battye, B. Garbrecht and A. Moss, *J. Cosmol. Astropart. Phys.* **09**, 007 (2006) [astro-ph/0607339];
R. Battye, B. Garbrecht and A. Moss, arXiv:1001.0769.
- [18] G. Lazarides and C. Pallis, *Phys. Lett. B* **651**, 216 (2007) [hep-ph/0702260];
G. Lazarides, *Int. J. Mod. Phys. A* **22**, 5747 (2007) [arXiv:0706.1436];
C. Pallis, *AIP Conf. Proc.* **1122**, 368 (2009) [arXiv:0812.0249].
- [19] C. Pallis, "High Energy Physics Research Advances", edited by T.P. Harrison and R.N. Gonzales (Nova Science Publishers Inc., New York, 2008) [arXiv:0710.3074].
- [20] V.N. Şenoğuz and Q. Shafi, *Phys. Lett. B* **668**, 6 (2008) [arXiv:0806.2798].
- [21] M. Ur Rehman, Q. Shafi and J.R. Wickman, *Phys. Rev. D* **79**, 103503 (2009) [arXiv:0901.4345].

- [22] L. Boubekeur and D. Lyth, *J. Cosmol. Astropart. Phys.* **07**, 010 (2005) [hep-ph/0502047];
K. Kohri, C.M. Lin and D.H. Lyth, *J. Cosmol. Astropart. Phys.* **12**, 004 (2007) [arXiv:0707.3826];
C.M. Lin and K. Cheung, *J. Cosmol. Astropart. Phys.* **03**, 012 (2009) [arXiv:0812.2731].
- [23] S.R. Coleman and E.J. Weinberg, *Phys. Rev. D* **7**, 1888 (1973).
- [24] Y. Watanabe and E. Komatsu, *Phys. Rev. D* **75**, 061301 (2007) [gr-qc/0612120];
Y. Watanabe and E. Komatsu, *Phys. Rev. D* **77**, 043514 (2008) [arXiv:0711.3442].
- [25] E.W. Kolb and M.S. Turner, *The Early Universe, Redwood City, USA: Addison-Wesley (1990)*.
- [26] K. Maeda, *Phys. Rev. D* **39**, 3159 (1989);
S. Kalara, N. Kaloper and K.A. Olive, *Nucl. Phys.* **B341**, 252 (1990);
V. Faraoni, E. Gunzig and P. Nardone, *Fund. Cosmic Phys.* **20**, 121 (1999) [gr-qc/9811047];
S. Carloni, E. Elizalde and S. Odintsov, arXiv:0907.3941.
- [27] G. Lazarides, *J. Phys. Conf. Ser.* **53**, 528 (2006) [hep-ph/0607032];
D. Baumann, arXiv:0907.5424.
- [28] D.S. Salopek, J.R. Bond and J.M. Bardeen, *Phys. Rev. D* **40**, 1753 (1989);
F. Bauer and D.A. Demir, *Phys. Lett. B* **665**, 222 (2008) [arXiv:0803.2664];
N. Makino and M. Sasaki, *Prog. Theor. Phys.* **86**, 103 (1991);
R. Fakir, S. Habib and W. Unruh, *Astrophys. J.* **394**, 396 (1992);
D.I. Kaiser, *Phys. Rev. D* **52**, 4295 (1995) [astro-ph/9408044].
- [29] C. Pallis, *Nucl. Phys.* **B751**, 129 (2006) [hep-ph/0510234];
C. Pallis, *Nucl. Phys.* **B831**, 217 (2010) [arXiv:0909.3026].
- [30] N. Sugiyama and T. Futamase, *Phys. Rev. D* **81**, 023504 (2010).
- [31] N. Bartolo, E. Komatsu, S. Matarrese and A. Riotto, *Phys. Rept.* **402**, 103 (2004) [astro-ph/0406398];
X. Chen, arXiv:1002.1416.
- [32] A.D. Linde, *Particle Physics and Inflationary Cosmology, Harwood, Chur, Switzerland, (1990)* [hep-th/0503203];
A.D. Linde, *Lect. Notes Phys.* **738**, 1 (2008) [arXiv:0705.0164].
- [33] R. Fakir and W.G. Unruh, *Phys. Rev. D* **41**, 1783 (1990);
E. Komatsu and T. Futamase, *Phys. Rev. D* **59**, 064029 (1999) [astro-ph/9901127].
- [34] <http://www.rssd.esa.int/SA/PLANCK/include/report/redbook/redbook-science.htm>
- [35] D.H. Lyth, *Phys. Rev. Lett.* **78**, 1861 (1997) [hep-ph/9606387];
R. Easther, W.H. Kinney and B.A. Powell, *J. Cosmol. Astropart. Phys.* **08**, 004 (2006) [astro-ph/0601276].
- [36] T.W.B. Kibble, *J. Phys. A* **9**, 387 (1976).
- [37] V. Faraoni, *Phys. Rev. D* **53**, 6813 (1996) [astro-ph/9602111];
S. Koh, S.P. Kim and D.J. Song, *Phys. Rev. D* **72**, 043523 (2005) [astro-ph/0505188].
- [38] G. Lazarides and Q. Shafi, *Phys. Lett. B* **258**, 305 (1991);
G. Lazarides, R.K. Schaefer and Q. Shafi, *Phys. Rev. D* **56**, 1324 (1997) [hep-ph/9608256].
- [39] K. Hamaguchi, *Phd Thesis* [hep-ph/0212305];
W. Buchmuller, R. D. Peccei and T. Yanagida, *Ann. Rev. Nucl. Part. Sci.* **55**, 311 (2005) [hep-ph/0502169].
- [40] M.B. Einhorn and D.R.T. Jones, arXiv:0912.2718.